The Journal of Immunology

The Hypervirulent *Mycobacterium tuberculosis* Strain HN878 Induces a Potent TH1 Response followed by Rapid Down-Regulation

Diane Ordway, Marcela Henao-Tamayo, Marisa Harton, Gopinath Palanisamy, Jolynn Troudt, Crystal Shanley, Randall J. Basaraba and Ian M. Orme

J Immunol 2007; 179:522-531; ;
doi: 10.4049/jimmunol.179.1.522
http://www.jimmunol.org/content/179/1/522

The Journal of Immunology is published twice each month by
The American Association of Immunologists, Inc.,
1451 Rockville Pike, Suite 650, Rockville, MD 20852

Print ISSN: 0022-1767 Online ISSN: 1550-6606.

The Hypervirulent *Mycobacterium tuberculosis* Strain HN878 Induces a Potent TH1 Response followed by Rapid Down-Regulation[1]

Diane Ordway,[2] Marcela Henao-Tamayo, Marisa Harton, Gopinath Palanisamy, Jolynn Troudt, Crystal Shanley, Randall J. Basaraba, and Ian M. Orme

The HN878 strain of *Mycobacterium tuberculosis* is regarded as "hypervirulent" due to its rapid growth and reduced survival of infected mice when compared with other clinical isolates. This property has been ascribed due to an early increase in type I IFNs and a failure to generate TH1-mediated immunity, induced by a response to an unusual cell wall phenolic glycolipid expressed by the HN878 isolate. We show, however, that although type I IFN does play an inhibitory role, this response was most apparent during the chronic disease stage and was common to all *M. tuberculosis* strains tested. In addition, we further demonstrate that the HN878 infection was associated with a potent TH1 response, characterized by the emergence of both CD4 and CD8 T cell subsets secreting IFN-γ. However, where HN878 differed to the other strains tested was a subsequent reduction in TH1 immunity, which was temporally associated with the rapid emergence of a $CD4^+CD25^+FoxP3^+CD223^+IL\text{-}10^+$ regulatory T cell population. This association may explain the paradoxical initial emergence of a TH1 response in these mice but their relatively short time of survival. *The Journal of Immunology,* 2007, 179: 522–531.

It is becoming apparent that a significant percentage of new clinical isolates of *Mycobacterium tuberculosis* are of high virulence (1, 2). Initial studies by Manca et al. (3, 4) demonstrated that the HN878 strain is of unusually high virulence, wherein mice failed to induce a strong TH1 T cell and cytokine response early in infection and died more rapidly in comparative survival studies. This "hypervirulence" was hypothesized to be associated with induction of increased production of type I IFN (4), and further work has subsequently shown that HN878 expresses a TH2 cytokine inducing biologically active phenolic glycolipid Ag in its cell wall, removal of which ablates its lethality (5).

The role of type I IFNs in the protective immune response to *M. tuberculosis* infection is not well understood. More recent reports from Manca et al. (3, 4) demonstrated that wild-type HN878-infected mice treated with anti-IFN-$\alpha\beta$ Ab results in higher TH1 cytokine response and increased survival of animal without concomitant differences in bacterial growth. Taken together, these studies suggested that the increased type I IFNs during infection with HN878 may be deleterious for survival of *M. tuberculosis*-infected mice, which was associated with reduced TH1 immunity (3, 4).

Cell-mediated immunity is responsible for control of tuberculosis (6, 7). After pulmonary infection of the mouse with *M. tuberculosis* (~50–100 CFU), alveolar macrophages and dendritic cells (DCs)[3] phagocytose the bacilli and DCs carry Ags to draining lymph nodes where recognition by T cells generates cell-mediated immunity (6–9). The generation of prolonged immunity to the products of the phagocytosed bacteria have Ags that are presented by macrophages, as Ag bound to class I MHC molecules to $CD8^+$, class II MHC molecules to $CD4^+$, and non-MHC molecules to $\gamma\delta^+$ T cells (10–13). The presentation of these molecules to T cells causes the secretion of IFN-γ, IL-12, and the subsequent signaling from TNF-α results in the activation of other macrophages to phagocytose and kill the intracellular organism (8, 12, 13). The additional influx of monocytes, macrophages, B cells, and neutrophils form the granulomatous lesion at the site of mycobacterial replication (14–17) in the lung to contain multiplication and further dissemination of the bacteria to other cells. Although there is an initial presence of a strong TH1 Ag-specific response in mice, which leads to the control of *M. tuberculosis* growth, these responses may also increase inflammation and lung immunopathology. Although the immunosuppressive cytokines such as TGF-β, IL-4, and IL-10 (9, 18, 19) are generally considered to increase the susceptibility to intracellular pathogens, their expression with a bacterial strain of higher virulence may be necessary to attenuate the potentially tissue-damaging inflammatory response (18–20). An example, of reduction of inflammatory tissue damage is the development of a CD4 T regulatory population that expresses CD25, CD223, and FoxP3, which down-regulates inflammation and protective TH1 responses (21, 22).

Materials and Methods

Mice

Specific pathogen-free female C57BL/6 mice were purchased from The Jackson Laboratory. Mice lacking the IFN-$\alpha\beta$ receptor on a 129 background were bred in-house at Colorado State University (Fort Collins, CO) from breeders provided by Dr. P. Marrack (National Jewish Medical and Research Center, Denver, CO). Mice were used at ~6–8 wk of age. Mice were maintained in the Biosafety Level 3 biohazard facility at Colorado State University, and were given sterile water, mouse chow, bedding, and

Mycobacteria Research Laboratories, Department of Microbiology, Immunology and Pathology, Colorado State University, Fort Collins, CO 80523

Received for publication January 26, 2007. Accepted for publication April 25, 2007.

The costs of publication of this article were defrayed in part by the payment of page charges. This article must therefore be hereby marked *advertisement* in accordance with 18 U.S.C. Section 1734 solely to indicate this fact.

[1] This work was supported by Grants AI-44072 and AI-40488 from the National Institutes of Health.

[2] Address correspondence and reprint requests to Dr. Diane Ordway, Department of Microbiology, Immunology and Pathology, Colorado State University, Fort Collins, CO 80523-1682. E-mail address: D.Ordway-Rodriguez@colostate.edu

[3] Abbreviations used in this paper: DC, dendritic cell; pDC, plasmacytoid DC; FSC, forward light scatter; SSC, side light scatter; GITR, glucocorticoid-induced TNF-related receptor; KO, knockout.

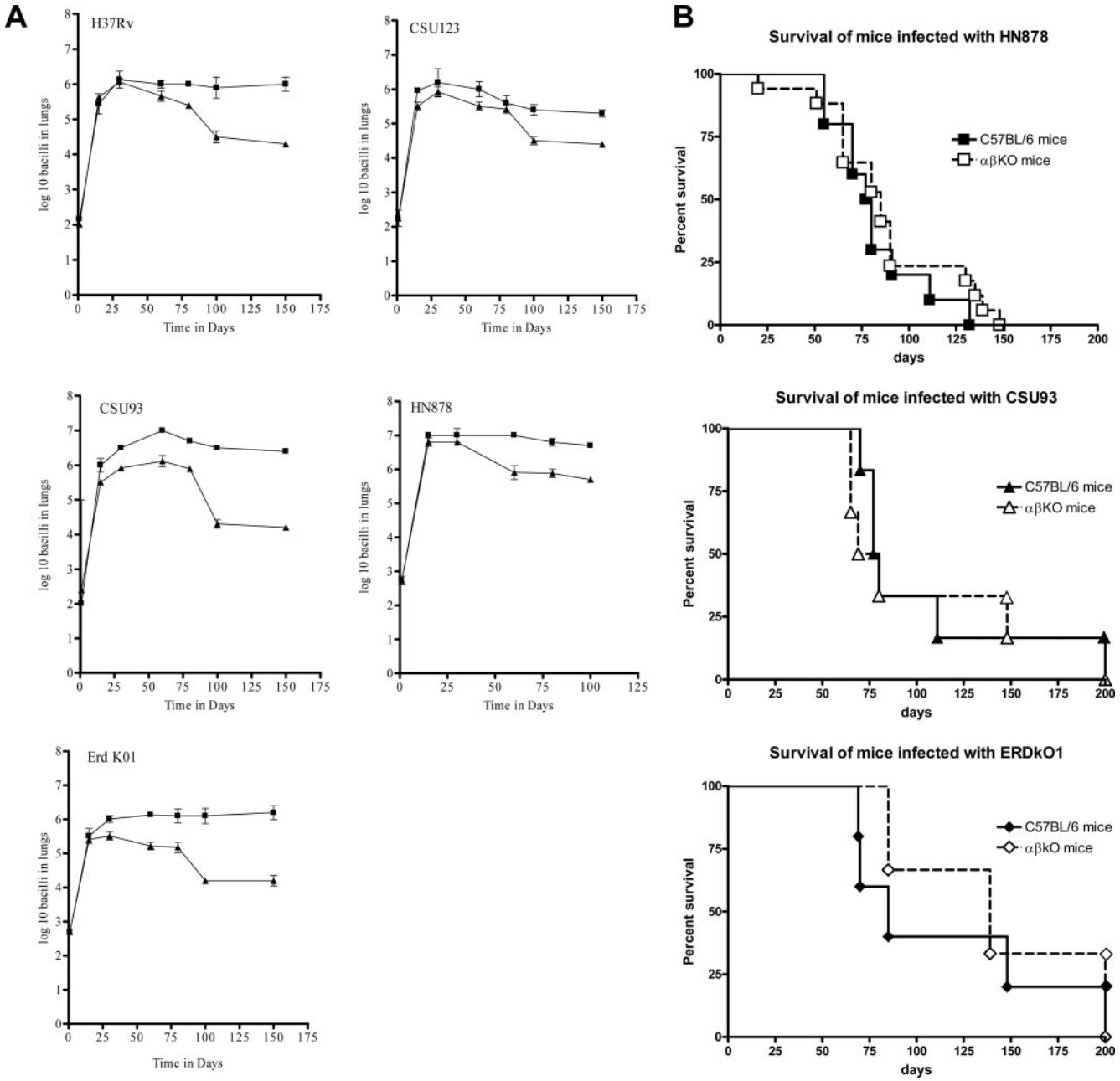

FIGURE 1. Decreased bacterial growth during chronic infection in the lungs of IFN-$\alpha\beta$ receptor KO mice. *A*, Bacterial counts in the lungs in C57BL/6 (■) and IFN-$\alpha\beta$ receptor KO (▲) mice infected with a low dose of *M. tuberculosis* strain H37Rv, CSU 123, CSU 93, HN878, or Erdman-KO1. Results are expressed as the mean ± SEM of the bacterial load in each group expressed as $\log_{10}$ CFU ($n = 5$ mice). *B*, Survival of C57BL/6 (filled symbols) and IFN-$\alpha\beta$ receptor KO (open symbols) mice infected with *M. tuberculosis* CSU 93, HN878, and Erdman-KO1. Survival results are from 10 mice per group.

enrichment for the duration of the experiments. The specific pathogen-free nature of the mouse colonies was demonstrated by testing sentinel animals. All experimental protocols were approved by the Animal Care and Use Committee of Colorado State University.

Experimental infections

Mice were challenged by low-dose aerosol exposure with *M. tuberculosis* using a Glas-Col aerosol generator calibrated to deliver 50–100 CFU of bacteria into the lungs. Information regarding preparation of bacterial stocks and growth characteristics of the various bacterial strains ($n = 5$) used were as previously described (1, 2). Strain H37Rv was originally obtained from the Trudeau Institute Collection; HN878 was provided by Dr. B. Kreiswirth (Public Health Research Institute Center, Newark, NJ); CSU 123 was provided by Dr. R. Cho, (Seoul, South Korea); CDC1551 (CSU 93) was provided by Dr. T. Shinnick (Centers for Disease Control and Prevention, Atlanta, GA); and Erdman-KO1 was obtained from Mycos Research, with permission from the Aeras Foundation.

Bacterial counts in the lung ($n = 5$ represents 5 mice and 5 lung samples) were determined by plating serial dilutions of organ homogenates on nutrient 7H11 agar and counting CFU after 3 wk incubation at 37°C. Lungs from mice ($n = 5$) in the same groups were harvested for histological analysis, and lung cell suspensions were used for flow cytometric analysis at indicated time points. In survival studies, animals showing substantial weight loss with no evidence of weight rebound were euthanized. The results shown in the survival studies are based upon 10 mice per group.

Histological analysis

The accessory lung lobe from each mouse was fixed with 10% Formalin in PBS. Sections from these murine tissues were stained using H&E, and by acid fast staining to detect mycobacteria.

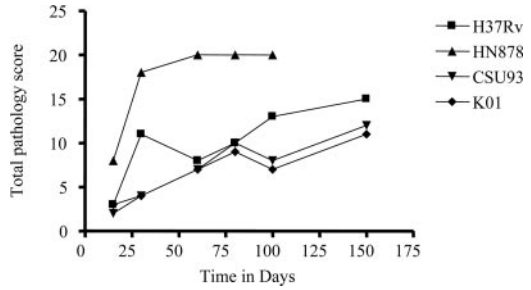

FIGURE 2. Increased total pathology scores in C57BL/6 mice infected with *M. tuberculosis* strain HN878. Sections of Formalin-fixed and paraffin-embedded lung tissue from mice infected with *M. tuberculosis* strains H37Rv (■), HN878 (▲), CSU 93 (▼), and Erdman-KO1 (♦) were stained with H&E and then added to give the total lesion score. Lesions were ranked in order of severity from 1 to 5 and scored for granuloma formation, alveolitis, perivasculitis, and peribroncholitis and the total scores were calculated.

Lung cell digestion

To prepare single-cell suspensions the lungs were perfused with a solution containing PBS and heparin (50 U/ml; Sigma-Aldrich) through the pulmonary artery and aseptically removed from the pulmonary cavity, placed in medium, and dissected. The dissected lung tissue was incubated with complete DMEM containing collagenase XI (0.7 mg/ml; Sigma-Aldrich) and type IV bovine pancreatic DNase (30 μg/ml; Sigma-Aldrich) for 30 min at 37°C. The digested lungs were further disrupted by gently pushing the tissue through a cell strainer (BD Biosciences). RBC were lysed with ACK buffer, washed, and resuspended in complete DMEM. Total cell numbers per lung were determined using a hemocytometer.

Flow cytometric analysis of cell surface markers

Cells suspensions from each individual mouse were incubated with mAbs labeled with FITC, PE, PerCP, or allophycocyanin at 4°C for 30 min in the dark. After washing the cells with deficient RPMI 1640 (Irvine Scientific) containing 0.1% sodium azide (Sigma-Aldrich), the cells were incubated with mAbs. Monoclonal Abs against $CD4^+$ (clone RM4-5, rat IgG2a,k), NK-1.1 (clone PK136, mouse IgGB2a,k), CD8 (clone 53-6.7, rat IgGB2a,k), CD3 (clone 145-2C11, Armenian hamster IgGB1,k), CD11c (clone HL3, hamster IgG1), CD11b (Mac-1, clone M1/70, rat IgG2a), Ly-6C/Gr1 (RB6-8C5, rat IgG2b), CD45R/B220 (RA3-6B2, rat IgG2a,k), CD25 (3C7, rat IgM), CD223 (C9B7W, rat IgG1), glucocorticoid-induced TNF-related receptor (GITR, DTA-1, rat IgG2b), markers, and rat IgG2a, rat IgG2b, rat IgG1, mouse IgG2a, and hamster IgG were used in this study. These mAbs were purchased from BD Pharmingen, Serotec, or eBioscience (San Diego, CA) as direct conjugates to FITC, PE, PerCP, PerCP-Cy5.5, Pacific blue, Pacific orange, or allophycocyanin. Data acquisition and analysis were done using FACSCalibur (BD Biosciences) and CellQuest software (BD Biosciences), respectively, or samples were examined with a LSRII flow cytometer (BD Biosciences) and data were analyzed using the FACSDiva software (BD Biosciences). Compensation of the spectral overlap for each fluorochrome was done using CD4 or CD11b Ags from cells gated in the forward light scatter $(FSC)^{low}$ vs side light scatter $(SSC)^{low}$ or $FSC^{mid/high}$ vs $SSC^{mid/high}$ region, respectively. Analyses were performed with an acquisition of at least 100,000 or 500,000 total T cell events and a minimum of 10,000 $CD11c^+$ events.

Intracytoplasmic cytokine staining

Cells were first stained for cell surface markers as indicated and thereafter the same cell suspensions were prepared for intracellular staining. Staining for markers of the Foxp3, IFN-γ, IL-10, granzyme B family was performed using an intracellular staining technique. Cell membranes were permeabilized according to the kit instructions (Fix/Perm kit; BD Pharmingen). Abs against Foxp3 (FJK-16s, rat IgG2a), IFN-γ (XMG1.2, rat IgG1; eBioscience), and IL-10 (JES5-16E3, rat TgG2b) were incubated with the appropriate surface-stained cells for 30 min, and the cells were washed twice and resuspended in deficient RPMI 1640 before analysis.

Inflammatory cytokine measurement

A cytometric bead array kit (BD Biosciences) was used to measure inflammatory cytokines of lung cell suspensions incubated for 72 h at 37°C with culture filtrate proteins at 2 μg/ml and then frozen at −80°C. After thawing the supernatants, the cytometric bead array mouse inflammatory cytokine assay procedure was performed according to kit instructions. Assays were completed with duplicate samples and results are expressed as the mean of two experiments. Values are represented by the mean cytokine in picograms per milliliter minus the noninfected medium control. The beads were analyzed on a BD Biosciences FACSCalibur flow cytometer.

Statistical analysis

Data are presented using the mean values ($n = 5$) using replicated samples and duplicate or triplicate assays. The parametric Student t test was used to assess statistical significance between groups of data.

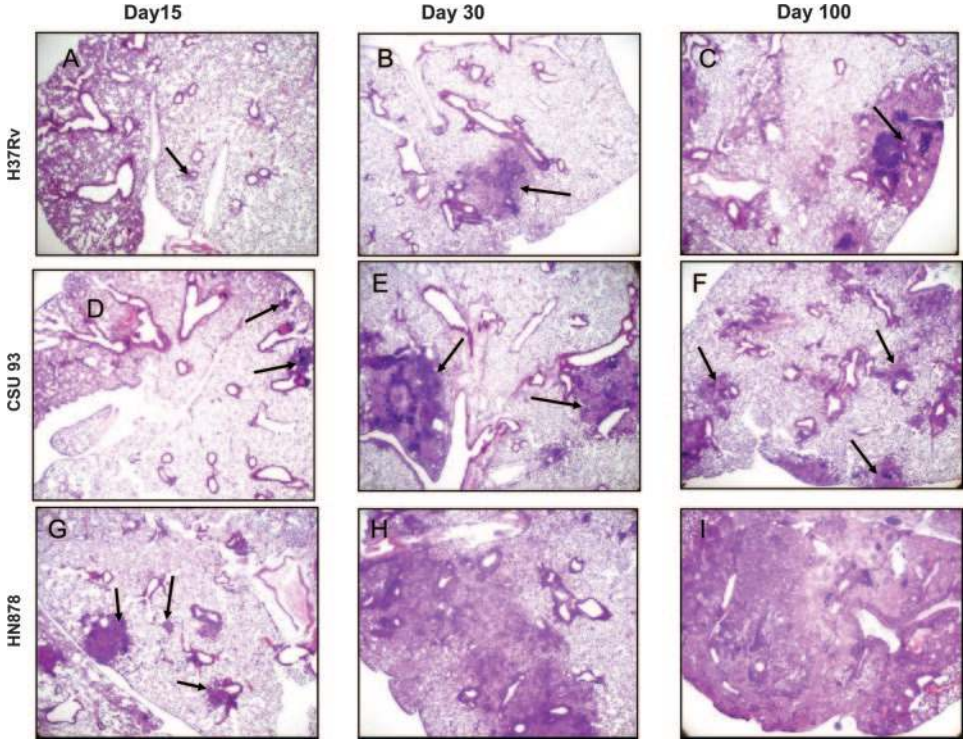

FIGURE 3. Increased lung pathology in C57BL/6 mice infected with *M. tuberculosis* strains. Sections of Formalin-fixed and paraffin-embedded lung tissue from mice infected with *M. tuberculosis* strains H37Rv (*A*, *B*, and *C*), CSU 93 (*D*, *E*, and *F*), and HN878 (*G*, *H*, and *I*) on days 15, 30, and 100 after *M. tuberculosis* challenge were compared. Lesions (arrow) were more numerous and larger in *M. tuberculosis* HN878-infected (*G*, *H*, and *I*) mice than in *M. tuberculosis* H37Rv-infected (*A*, *B*, and *C*) mice, eventually resulting in complete lung consolidation (*I*). *M. tuberculosis* CSU 93 (*D*, *E*, and *F*) induced smaller lesions in terms of size compared with *M. tuberculosis* H37Rv infection, but at an increased number of lesions. Total original magnification, ×10.

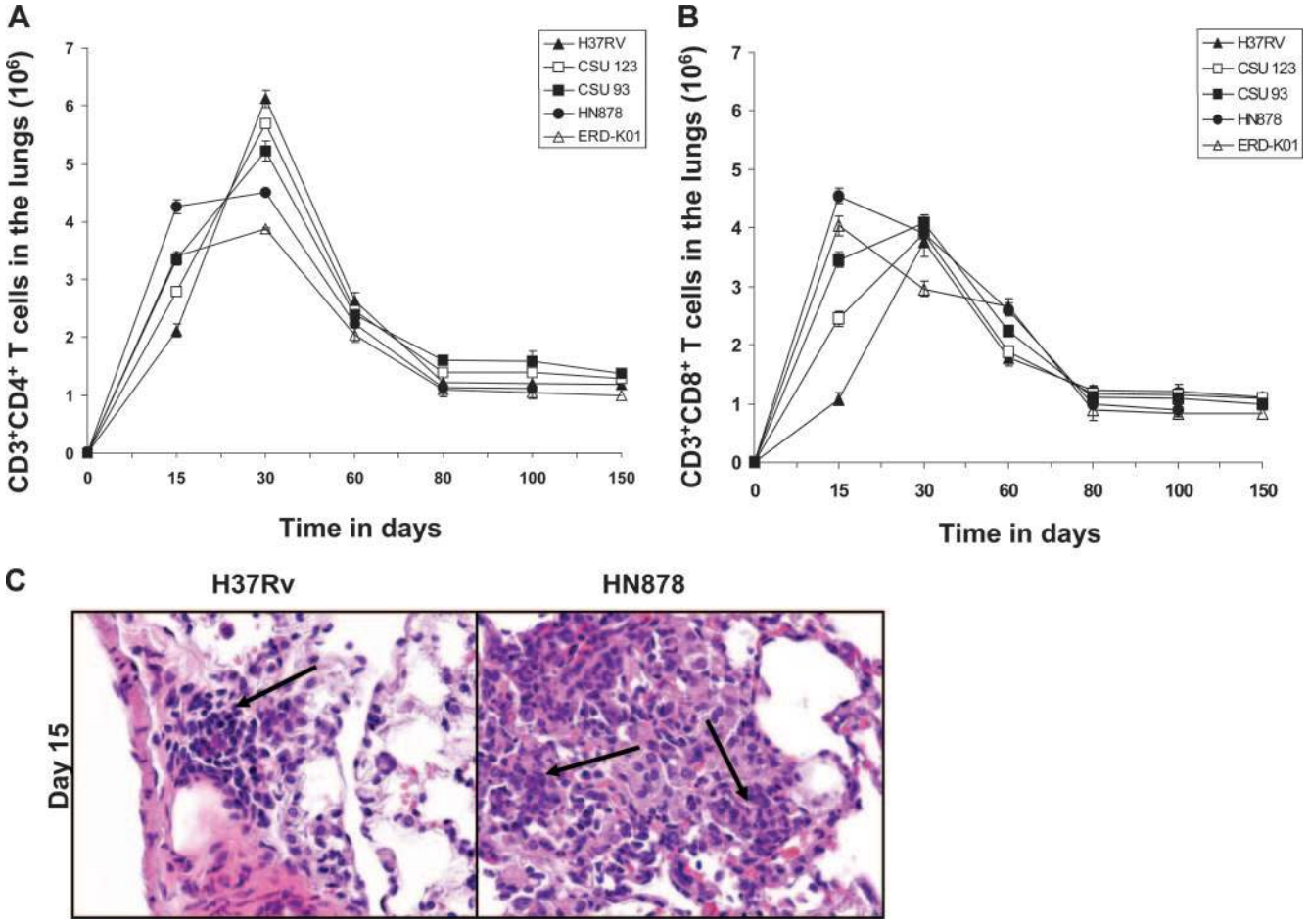

FIGURE 4. Early infiltration of $CD4^+$ and $CD8^+$ T cells in the lungs of mice infected with *M. tuberculosis* strains. Lung cells obtained from C57BL/6 mice infected with a low dose of *M. tuberculosis* strains H37Rv (▲), CSU 123 (□), CSU 93 (■), HN878 (●), and Erdman-KO1 (△) were assayed by flow cytometry. *A*, The total number of cells expressing $CD3^+CD4^+$ surface markers. *B*, $CD3^+CD8^+$ surface markers in the lungs of mice infected with the various strains of *M. tuberculosis*. Results are expressed as the average ± SEM ($n = 5$ mice) number of $CD3^+CD4^+$ or $CD3^+CD8^+$ T cells in the lungs. *C*, Mice infected with *M. tuberculosis* HN878 (*right*) demonstrated a substantial increase in lymphocytes accumulating in lesions (arrow) compared with *M. tuberculosis* H37Rv infection (*left*).

Results

Comparison of survival and lung bacterial loads in the lungs of C57BL/6 and IFN-αβ receptor KO mice infected with virulent strains of M. tuberculosis

In a first study we compared the growth of each of the five test strains in the lungs of mice exposed to low-dose aerosol infection (Fig. 1*A*). In the case of H37Rv, CSU 123, and Erdman-KO1, all showed evidence of slowing when reaching $\sim 10^6$ bacteria in the lungs, whereas levels of CSU 93 continued to rise, peaking at 10^7 after day 50. In contrast, HN878 grew faster than the other strains, reaching a lung bacterial load of 10^7 by as early as day 15 before showing evidence of containment.

A second study comparing the survival times of mice infected with the panel of laboratory and clinical strains was consistent with the resulting data and confirmed earlier reports (4, 5), illustrating the much higher virulence of the HN878 strain (Fig. 1*B*).

These studies also addressed the previous hypothesis (4) that this virulence reflected the production of type I IFN by comparing the growth of HN878 in control mice with IFN-αβ receptor gene disrupted knockout (KO) mice. We found this hypothesis to be the case, with better control of the bacterial load in mice unable to make type I IFN (Fig. 1*A*). However, this possibility was not restricted to HN878, but was a common observation with all five strains tested. Moreover, whereas an earlier report (4) implied that these cytokines had an early influence, the data obtained from the IFN-αβ KO mice showed that the inhibitory effects of these cytokines was predominantly expressed during the chronic stage of the disease process.

Differences in the granulomatous response in the lungs

We then examined the lung pathology in the HN878 mice and compared it with pathology found in mice with the other infections. Lesions were ranked in order of severity from 1 to 5 and scored for granuloma formation, alveolitis, perivasculitis, and peribroncholitis. All parameters were added for a total score. As shown in Fig. 2, the rapid growth of HN878 was associated with substantial lung damage, whereas the pathology scores rose much more slowly in lungs with the other infections. Interestingly, lung damage in the HN878-infected mice clearly slowed after day 30.

Lung pathology is also illustrated in Fig. 3, which shows the appearance of the lung tissues in mice infected with HN878 compared with animals infected with H37Rv or CSU 93. Examination of the lungs of C57BL/6 mice 15 days after being given a low-dose aerosol infection showed small aggregates of cells (Fig. 3*A*). By day 30, moderately sized lesions present, which consisted predominantly of macrophages and large aggregates of lymphocytes, were

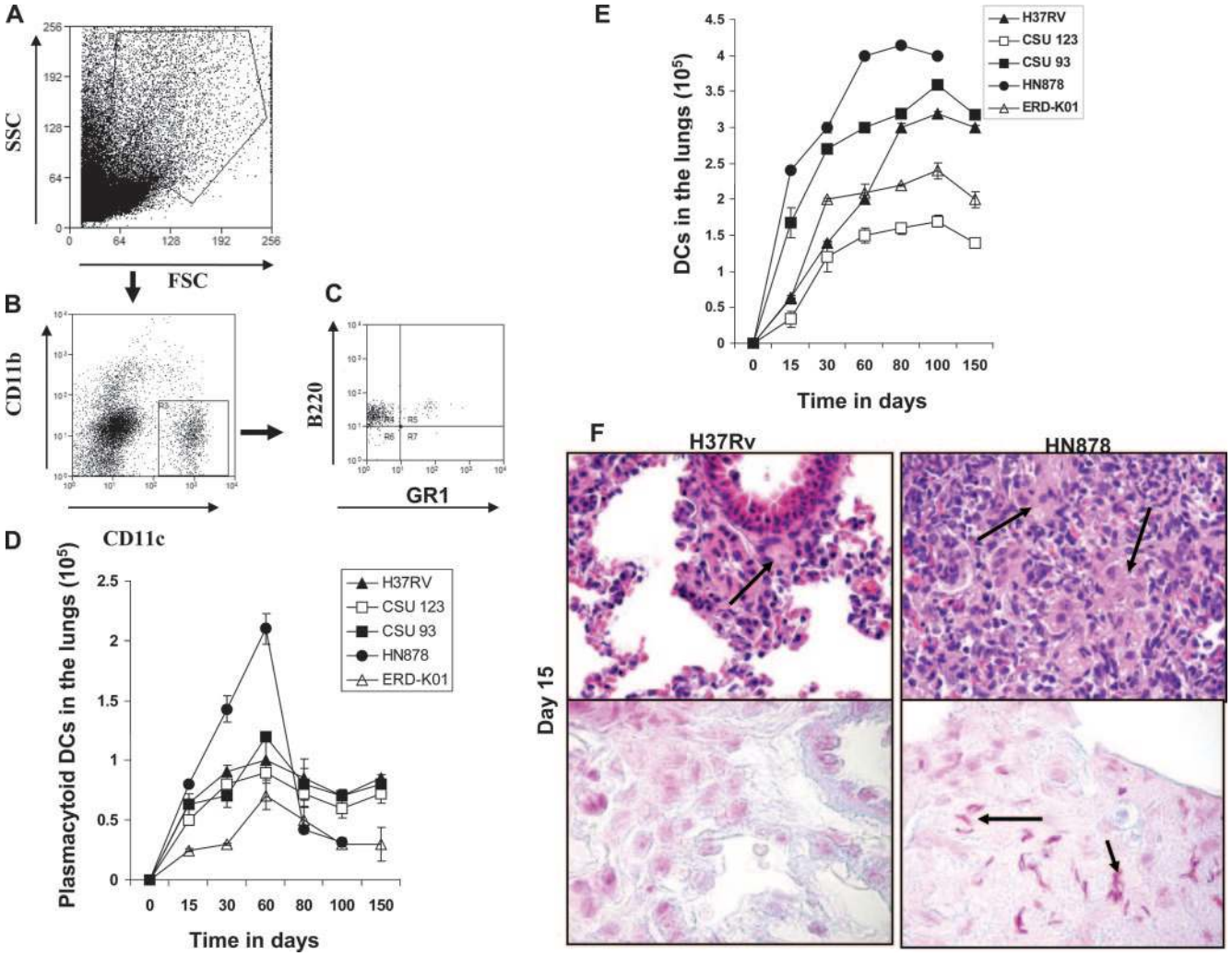

FIGURE 5. Early infiltration of DCs and pDCs in the lungs of mice infected with *M. tuberculosis* strains HN878 and CSU 93. *A*, A representative dot plot of lung cells from a representative mouse primarily gated on FSC^{high} vs SSC^{high} granulocytes. *B* and *C*, Then gating on DCs by gating on the region containing $CD11b^{-}CD11c^{+}GR1^{-}$ $CD11b^{-}$ cells (*B*) and on pDCs by gating on the region $CD11b^{-}CD11c^{+}B220^{+}Gr1^{+}$ cells (*C*). *D* and *E*, The lung cells obtained from C57BL/6 mice infected with a low dose of *M. tuberculosis* strains H37Rv (▲), CSU 123 (□), CSU 93 (■), HN878 (●), and Erdman-KO1 (△) were assayed by flow cytometry for the total number of pDCs (*D*) and DCs (*E*). Results are expressed as the average ± SEM number of ($n = 5$ mice) pCDs or DCs in the lungs. *F*, Mice infected with *M. tuberculosis* HN878 (*top right*) demonstrated a large number of highly vacuolated foamy cells (arrow) containing a large number of acid fast-positive staining bacilli (arrow) (*bottom right*) compared with *M. tuberculosis* H37Rv (*left panels*). H&E staining (*top*) and acid fast-positive staining (*bottom*) are shown. Total original magnification, ×20 (*top*) and ×100 (*bottom*).

seen within the epithelioid macrophage fields. The development of organized multifocal granulomas containing lymphocytes and macrophages progressed through day 100 (Fig. 3*C*). Infections with CSU 123 and Erdman-KO1 showed similar pathology (data not shown).

The development of pathology in the lungs of mice given CSU 93 was similar but more exaggerated. During early infection lesions tended to be larger than those seen with H37Rv and again consisted of aggregates of lymphocytes and some macrophages (Fig. 3*D*). Evidence for worsened lung pathology was apparent by day 30 (Fig. 3*E*) characterized by an increased number of lymphocytes and highly vacuolated cells infiltrating into the lung tissues resulting in large lesions. By day 100, however, the frequency of lesions and lung consolidation had appeared to stabilize (Fig. 3*F*).

Marked differences in pathology were seen in mice infected with *M. tuberculosis* HN878. Early in infection, moderately sized lesions were already developing, denoted by increased lymphocytic and phagocytic cellular infiltration, and thickening of the parenchymal walls indicative of inflammation in excess to the other strains tested (Fig. 3*G*). These lesions continued to increase in size as the infection progressed (Fig. 3*H*), characterized by coalescing inflammatory granulomas that were larger than those seen in the other groups. Most lesions contained a large number of highly vacuolated "foamy" macrophages containing a large number of acid fast bacilli. By day 100, most of the lung tissues were consolidated, with some lesions showing evidence of necrosis (Fig. 3*I*).

Differences in the influx of $CD4^{+}$ and $CD8^{+}$ T cells in the lungs of infected mice

Given the clear differences seen in cell influx indicated by the histological analysis, we conducted a comparative flow cytometric analysis of $CD4^{+}$ and $CD8^{+}$ T cell populations in lung cell digests from each group of infected mice. T cells were gated with a primary gate on viable FSC^{low} vs SSC^{low} lymphocytes and then

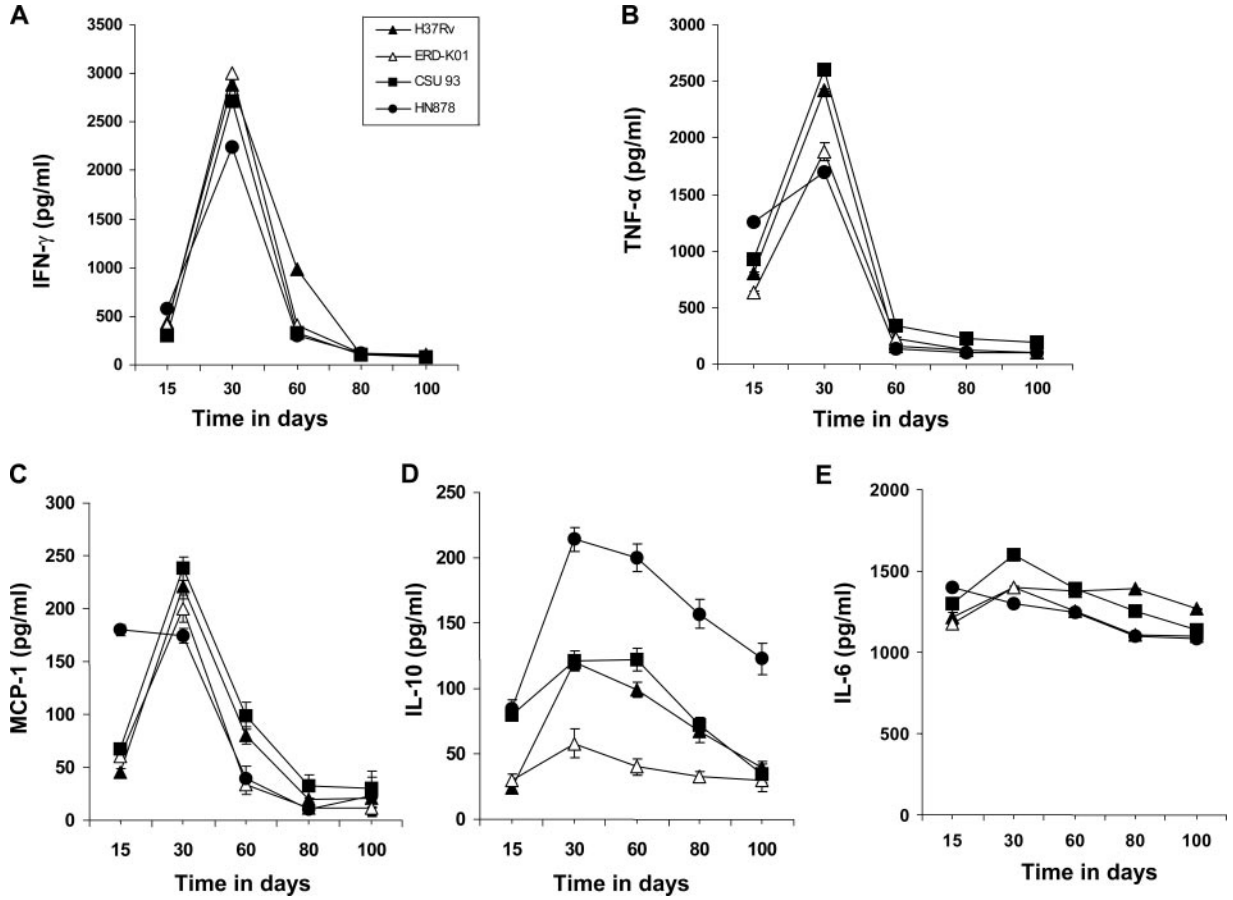

FIGURE 6. Differential production of IFN-γ, TNF-α, MCP-1, IL-10, and IL-6 cytokines by lung cells from C57BL/6 mice exposed to various virulent strains of *M. tuberculosis*. Inflammatory cytokine responses in the lung after cells were isolated from mice infected with a low dose of *M. tuberculosis* strains H37Rv (▲), Erdman-KO1 (△), CSU 93 (■), and HN878 (●) were incubated with culture filtrate proteins at 37°C and frozen after 72 h. Levels of IFN-γ (*A*), TNF-α (*B*), MCP-1 (*C*), IL-10 (*D*), and IL-6 (*E*) were measured using a inflammatory cytometric bead array kit. Results are expressed as the mean ± SEM (in picograms per milliliters, $n = 5$ mice) in the lungs.

on $CD3^+$ T cells, and analyzed for changes in the total percentage of $CD3^+CD4^+$ and $CD3^+CD8^+$ cells over the course of infection (Fig. 4).

In mice infected with HN878, there were rapid influxes of both CD4 and CD8 cells (Fig. 4, *A* and *B*), reaching higher levels on day 15 of the infection compared with the other four strains. This stabilized by day 30 and then declined at a similar rate in all groups. These observations were consistent with histological data from day 15, in which much larger lymphocytic lesions were observed in the animals infected with HN878 (Fig. 4*C*).

Differences in the influx of DCs and plasmacytoid DCs (pDCs) in the lungs of infected mice

DCs and pDCs are major producers of type I IFNs that are involved in inflammation, immunoregulation, and T cell responses during bacterial and viral infections (43–45). Given earlier reports implicating increased type I IFN in mice infected with *M. tuberculosis* HN878, we decided to monitor the number of pDCs and DCs infiltrating the lungs over the course of the disease.

The number of $CD11b^-CDllc^+B220^-Gr1^-$ DCs and $CD11b^-CDllc^+B220^+Gr1^+$ pDCs was determined by primarily gating on FSC^{high} vs SSC^{high} granulocytes (Fig. 5*A*) and then detecting DCs in the $CD11c^+$ region containing $CD11b^-CD11c^+$ cells (Fig. 5*B*), which also were $B220^-GR1^-$. Thereafter, pDCs were present in the region containing $CD11b^-CD11c^+GR1^+$ $CD11b^+$ cells (Fig. 5*C*).

As shown in Fig. 5*D*, the total number of pDCs in the lungs obtained from *M. tuberculosis* HN878-infected mice increased in much larger numbers from day 15 to day 60 of the infection compared with the number of pDCs in mice infected with other strains. Similarly, the total number of DCs in the lungs of HN878-infected mice steadily increased with time at a higher rate than seen in the other strains (Fig. 5*E*). In previous studies we have found evidence of DC markers on highly vacuolated foamy macrophages in granulomatous lesions (46), and so it was interesting to note in the current study that many more cells of this type appeared early in lesions in lungs of HN878-infected mice compared with H37Rv infection (Fig. 5*F*) and that these contained a large number of acid fast-positive bacteria (Fig. 5*F*).

Differential production of IFN-γ, TNF-α, MCP-1, IL-10, and IL-6 cytokines by cells from infected lungs

As shown in Fig. 6*A*, we were able to demonstrate that T cells harvested from the lungs of all infected groups and stimulated in vitro with culture filtrate proteins were able to produce IFN-γ, thus questioning earlier reports that HN878-infected mice could not generate a TH1 response. Further analysis of supernatants also revealed similar amounts of TNF-α, MCP-1, and IL-6 (Fig. 6, *B–E*). Interestingly, and consistent with further results described below, IL-10 production was considerably elevated in the HN878 group after day 30.

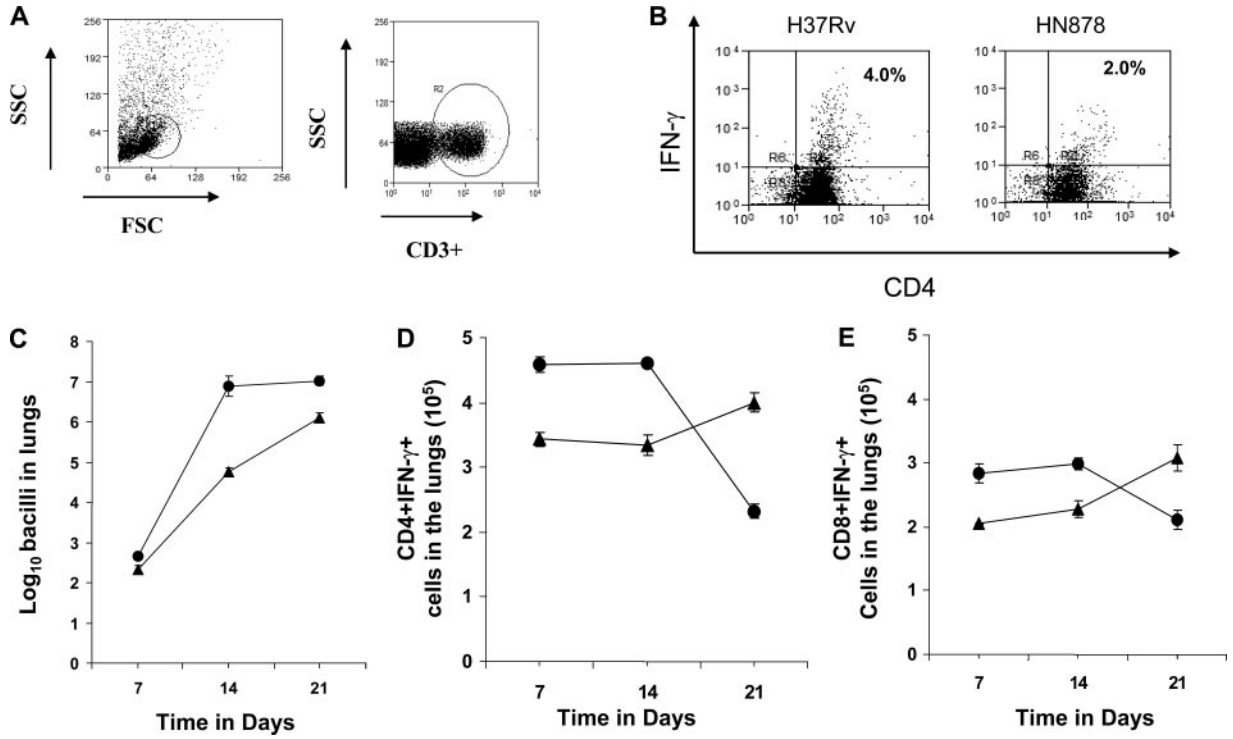

FIGURE 7. Early increase in the number of $CD4^+$ and $CD8^+$ IFN-γ^+ cells in HN878-infected mice. Mice were infected with a low dose of *M. tuberculosis* strains H37Rv or HN878 and then were assayed for bacterial loads (*C*) or by flow cytometry (*A*, *B*, *D*, and *E*) on days 7, 14, and 21. *A*, A representative dot plot of lung cells from a representative mouse after 21 days of infection with H37Rv (▲) or HN878 (●) primarily gated on viable FSC^{low} vs SSC^{low} lymphocytes (*A*) and then on $CD3^+$ T cells (*A*) and then gated on $CD4^+$ IFN-γ+ cells (*B*). *B*, The percentages shown represent H37Rv 4.0% of $CD4^+$IFN-γ cells and HN878 2.0% of $CD4^+$IFN-γ cells. *C*, Increased bacterial counts ± SEM in the lungs of mice infected with HN878 compared with H37Rv infection ($n = 5$ mice). *D*, Increased number of $CD4^+$ cells expressing IFN-γ. *E*, Increased $CD8^+$ cells expressing IFN-γ in the lungs of mice infected with HN878 compared with H37Rv. Results are expressed as the mean number ± SEM of $CD4^+$ and $CD8^+$ ($n = 5$ mice) IFN-γ^+ T cells in the lungs.

Characterization of $CD4^+$ and $CD8^+$ cells in the lungs of C57BL/6 mice exposed to M. tuberculosis *strains H37Rv or HN878 reveals the appearance of regulatory T cells in the latter group*

It was interesting to note that despite the rapid growth of the HN878 strain it was rapidly controlled by host immunity and quickly showed evidence of entering a chronic state. An initial rapid worsening of lung pathology also began to apparently stabilize, and these mice somewhat paradoxically showed evidence of increased IL-10 production. To try to understand these early events we performed studies in which we reexamined the early T cell response. Fig. 7 shows a representative dot plot of lung cells from a representative mouse after 21 days of infection with H37Rv or HN878 primarily gated on viable FSC^{low} vs SSC^{low} lymphocytes and then on $CD3^+$ T cells (Fig. 7*A*) and then gated on $CD4^+$ IFN-γ^+ cells (Fig. 7*B*). Fig. 7*C* shows the bacterial load in the lungs over the first 21 days and the number of IFN-γ-secreting CD4 or CD8 found in the lungs at that time. Fig. 7, *D* and *E*, shows an increased number of IFN-γ-secreting CD4 or CD8 T cells in the HN878-infected mice, but also evidence of a drop at day 21. We found evidence that initially HN878 induces a strong TH1 response characterized by significant IFN-γ production, which by day 14 begins to decline.

In view of this observation, we performed a much more comprehensive examination of the phenotypes of the CD4 and CD8 cells present in the lungs using multiparameter flow cytometry. The number of T cells was gated with a primary gate on viable FSC^{low} vs SSC^{low} lymphocytes (Fig. 8*A*) and then a gate on $CD4^+$ T cells (Fig. 8*B*) coexpressing CD25 and FoxP3 (Fig. 8*C*) and CD223 and IL-10 (Fig. 8*D*). Changes in the total percentage of these cells were monitored over the course of infection. To our surprise, we not only found evidence of CD4 cells expressing the regulatory T cell markers CD25, FoxP3, and CD223 in the lungs, but also evidence of a rapid expansion of these cells by day 21 (Fig. 8*E*). Moreover, many of these cells were also positive for intracellular IL-10 (Fig. 8*F*). A very low number of such cells was seen in the H37Rv-infected mice but with no evidence of any expansion (in our unpublished observations, we monitored mice infected with H37Rv for over 300 days and found no evidence for any expansion of CD4 cells with a regulatory T cell phenotype).

To further validate the presence of immunosuppressive T regulatory cells during infection with the HN878 strain, we evaluated expression of the mouse GITR. GITR interaction with its ligand augments T cell activation, proliferation, and IL-2, IFN-γ, and IL-4 cytokine secretion and abrogates regulatory T cell suppression (47–49). C57BL/6 mice infected with HN878 demonstrated an increased number of $CD4^+CD25^+GITR^+$ T cells in the lungs during the early course of infection compared with *M. tuberculosis* H37Rv-infected mice (Fig. 8*G*). However, C57BL/6 mice infected with *M. tuberculosis* H37Rv showed a substantial increase in $CD4^+$ $CD25^+GITR^+$ T cells in the lungs after 21 days of the infection. By this time, this population was declining in the HN878-infected mice indicative of reduced $CD4^+$ T cell proliferation and activation. GITR plays a key role in regulating the immunosuppressive function mediated by regulatory T cells. Therefore the increased expression of GITR by *M. tuberculosis* H37Rv-infected mice indicates a state of T cell activation and prevents the development of immunosuppressive T cells. In contrast, decreased expression of GITR by *M. tuberculosis* HN878-infected mice indicates removal of GITR signaling, which leads to the development of immunosuppressive T cells.

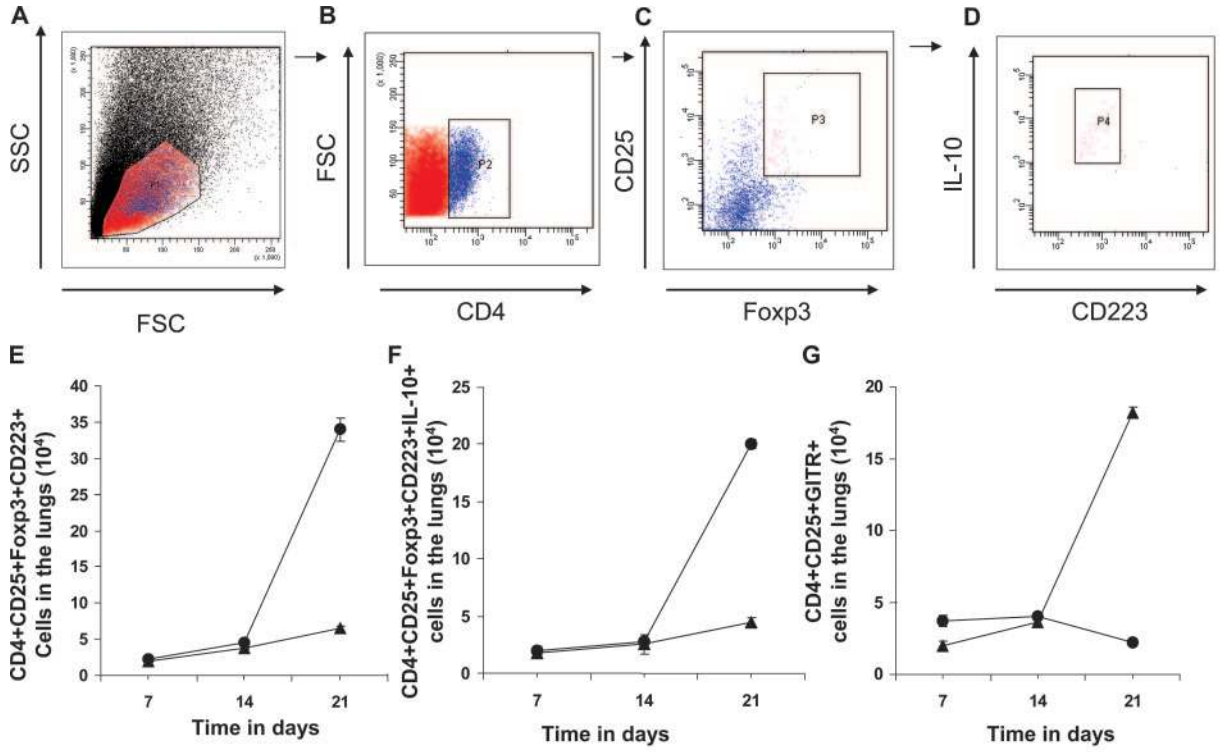

FIGURE 8. T cell activation decreased with the increased number of $CD4^+CD25^+Foxp3^+CD223^+IL\text{-}10^+$ cells in HN878-infected mice. Lung cells obtained from C57BL/6 mice infected with a low dose of *M. tuberculosis* strains H37Rv (▲) or HN878 (●) were assayed by multiparametric flow cytometry on days 7, 14, and 21. Representative dot plot of lung cells from a representative mouse primarily gated on viable FSC^{low} vs SSC^{low} lymphocytes (*A*, red) and then on $CD4^+$ T cells (*B*, blue), coexpressing CD25 and FoxP3 (*C*, green) and CD223 and IL-10 (*D*, pink). Mice infected with HN878 showed a substantial increase in $CD4^+CD25^+Foxp3^+CD223^+$ (*E*) and $CD4^+CD25^+Foxp3^+CD223^+IL\text{-}10^+$ (*F*) regulatory T cells in the lungs at 21 days of infection compared with H37Rv-infected mice. *G*, Mice infected with H37Rv had a significant increase in $CD4^+CD25^+GITR^+$ T cells in the lungs at 21 days of infection, whereas a negligible number was seen in HN878-infected mice. Results are expressed as the mean number ± SEM of $CD4^+CD25^+Foxp3^+CD223^+$, $CD4^+CD25^+Foxp3^+CD223^+IL\text{-}10^+$, or $CD4^+CD25^+GITR^+$ T cells ($n = 5$ mice) in the lungs.

Discussion

The results of this study show that the *M. tuberculosis* strain HN878 is clearly more virulent for mice than other strains, growing much faster in the lungs and inducing severe lung damage and consolidation. After 20–30 days or more, the infection is contained and the lung pathology apparently slows, but animals still die more quickly than other virulent strains. The reason for this paradox can hypothetically be explained by our observation that the HN878 infection rapidly induces progressive lung pathology during a time when the protective TH1 response declines, which was associated with the appearance of a regulatory T cell response. In our study, we show these forementioned events occurred during the same time frame and do not demonstrate a causal link between the lung pathology and the appearance of a regulatory T cell population during HN878 infection.

In this regard, we found evidence that initially HN878 induces a strong TH1 response, contrary to the hypothesis of Manca and colleagues (4, 5) who have argued that the hypervirulence of HN878 reflects its ability to avoid a TH1 response, an ability ascribed to its possession of a cell wall polyketide synthase-derived phenolic glycolipid that induces cytokines known to block TH1 responses (5). However, in our hands, HN878 induced a potent TH1 response characterized by significant IFN-γ and TNF-α production; this peaked by day 14 and then declined. It is possible that the differences in our results and the earlier reports from Manca and colleagues (4, 5) could be due to differences in the experimental methods used, as we tracked the early phenotypical cellular kinetics and cytokine responses by flow cytometry compared with their reports using RT-PCR for cytokine mRNA in the animals lungs. Furthermore, our report depended heavily on the animals lung pathology induced by the HN878 strain, whereas their studies were devoid of pathological analyses (4, 5).

Earlier studies also found evidence for an increased production of type I IFN and hypothesized that this interfered with the ability of the animal to control the infection (4). To test this further, we compared normal and IFN-$\alpha\beta$ receptor KO mice, reasoning that inability to respond to these cytokines would improve protection. This effect indeed seemed to be the case, but was only evident for most strains well into the chronic phase of the disease.

A steady increase in both pDCs and DCs was observed in the lungs of all the infection groups, and these cells are known to be rich sources of type I IFN (43, 50). The apparent lack of TH1 immunity during HN878 infection in earlier reports was associated with increases in IFN-α but changes in the levels of IFN-β were not evaluated. This observation is important because other reports have shown that infection of C57BL/6 mice with *Listeria* induces IFN-β expression and suppresses the accumulation of $CD11b^+$ macrophages secreting TNF-α cells at the sites of infection (51). In contrast IFN-$\alpha\beta$ receptor KO mice were more resistant to *Listeria* infection and had a greater number of $CD11b^+$ cells producing TNF-α and IL-12p70 cells at the site of infection (51). In the present study, pDCs and DCs were very prominent in the early response to HN878, and were found to be harboring a large number of acid fast bacilli. In addition, foamy cells, which express the

DC marker DEC-205, were also prominent; these cells down-regulate molecules involved in Ag presentation and may potentially provide safe niches for *M. tuberculosis* survival (46).

In our evaluation of the early T cell response in the HN878-infected mice, we observed that both CD4 and CD8 cells secreting IFN-γ were rapidly induced, but these began to decline at 21 days, whereas at the same time a rapid increase in IL-10$^+$ CD4 cells was observed. These latter cells stained positive for CD25, CD223, and FoxP3, which are all known markers of immunosuppressive regulatory T cells (27, 28). A recent report showed cotransferred CD4$^+$ CD25$^+$ T regulatory cells from naive C57BL/6 mice into C57BL/6J-Rag1$^{-/-}$ mice infected with *M. tuberculosis* H37Rv resulted in suppression of protective immunity, which was not associated with IFN-γ, inducible NO synthase, nor increased IL-10 (52). Our current study evaluated the early T regulatory cell response during *M. tuberculosis* H37Rv infection and supports the notion that the presence of T regulatory cells was not associated with inhibition of the early acquired immune response by reduced IFN-γ. It is probable that differences in the virulence and kinetics of the immunopathology induced by these two bacterial strains are associated with the degree to which functional characteristics of T regulatory cells are expressed.

In addition we evaluated the expression of GITR on T regulatory cells by *M. tuberculosis* HN878-infected mice, which was down-regulated by day 21 and associated with the appearance of immunosuppressive regulatory T cells (47–49). GITR is expressed at low levels on responder T cells and is up-regulated in T regulatory cells and in activated T cells (47). Activation of GITR enhances costimulation of responder T cells and suppressor activity is abrogated, resulting in enhanced immune responses (47–49). It is plausible that the reduced expression of GITR in *M. tuberculosis* HN878-infected mice evident by day 21 and coincided with reduced IFN-γ represents lack of GITR signaling and less potent T cell activation. In contrast *M. tuberculosis* H37Rv showed increased GITR expression, which was associated with increased IFN-γ expression (47).

Whether the speed of the emerging TH1 response was the stimulus for the induction of the regulatory T cell subset is unknown, but it was clearly much faster than that seen in the other *M. tuberculosis* infections, and indeed we have yet to detect this latter subset in these other cases (even high dose i.v. models). A second possibility is that regulatory T cells responded to the acute lung damage caused by the HN878 infection, consistent with our previous observation that IL-10, a product of regulatory T cells as well as macrophages, may play a role in maintaining the stability of chronic lung disease in the face of increasing necrosis (19). A similar observation has been made in the case of *Bordetella pertussis* infection (53). Moreover there is evidence that patients with active tuberculosis have raised levels of circulating regulatory T cells (22, 54). More importantly these tuberculosis patients demonstrated T regulatory cells were expanded at sites of active tuberculosis disease in parallel with high local concentrations of *M. tuberculosis*-specific TH1-type IFN-γ-secreting T cells and in areas of immunopathology (22). Future studies are warranted sorting these T regulatory cells and using adoptive cell transfer into C57BL/6J-Rag1 mice to show a causal link between the aggressive TH1 response and the appearance of immunosuppressive T regulatory cells during HN878 infection.

Disclosures

The authors have no financial conflict of interest.

References

1. Orme, I. M. 1999. Virulence of recent notorious *Mycobacterium tuberculosis* isolates. *Tuber. Lung Dis.* 79: 379–381.
2. Ordway, D. J., M. G. Sonnenberg, S. A. Donahue, J. T. Belisle, and I. M. Orme. 1995. Drug-resistant strains of *Mycobacterium tuberculosis* exhibit a range of virulence for mice. *Infect. Immun.* 63: 741–743.
3. Manca, C., L. Tsenova, S. Freeman, A. K. Barczak, M. Tovey, P. J. Murray, C. Barry, and G. Kaplan. 2005. Hypervirulent *M. tuberculosis* W/Beijing strains upregulate type I IFNs and increase expression of negative regulators of the Jak-Stat pathway. *J. Interferon Cytokine Res.* 25: 694–701.
4. Manca, C., L. Tsenova, A. Bergtold, S. Freeman, M. Tovey, J. M. Musser, C. E. Barry, III, V. H. Freedman, and G. Kaplan. 2001. Virulence of a *Mycobacterium tuberculosis* clinical isolate in mice is determined by failure to induce Th1 type immunity and is associated with induction of IFN-α/β. *Proc. Natl. Acad. Sci. USA* 98: 5752–5757.
5. Manca, C., M. B. Reed, S. Freeman, B. Mathema, B. Kreiswirth, C. E. Barry, III, and G. Kaplan. 2004. Differential monocyte activation underlies strain-specific *Mycobacterium tuberculosis* pathogenesis. *Infect. Immun.* 72: 5511–5514.
6. Orme, I. M. 1998. The immunopathogenesis of tuberculosis: a new working hypothesis. *Trends Microbiol.* 6: 94–97.
7. Flynn, J. L., and J. Chan. 2001. Immunology of tuberculosis. *Annu. Rev. Immunol.* 19: 93–129.
8. Flynn, J. L. 2006. Lessons from experimental *Mycobacterium tuberculosis* infections. *Microb. Infect.* 8: 1179–1188.
9. Rook, G. A., and R. Hernandez-Pando. 1996. The pathogenesis of tuberculosis. *Annu. Rev. Microbiol.* 50: 259–284.
10. Roach, D. R., A. G. D. Bean, C. Demangel, M. P. France, H. Briscoe, and W. J. Britton. 2002. TNF regulates chemokine induction essential for cell recruitment, granuloma formation, and clearance of mycobacterial infection. *J. Immunol.* 168: 4620–4627.
11. Orme, I. M., A. Roberts, J. Griffin, and J. Abrams. 1993. Cytokine secretion by CD4 T lymphocytes acquired in response to *Mycobacterium tuberculosis* infection. *J. Immunol.* 151: 518–525.
12. Cooper, A. M., J. Magram, J. Ferrante, and I. M. Orme. 1997. IL-12 is crucial to the development of protective immunity in mice intravenously infected with *Mycobacterium tuberculosis*. *J. Exp. Med.* 186: 39–46.
13. Flynn, J. L., M. M. Goldstein, K. J. Triebold, J. Sypek, S. Wolf, and B. R. Bloom. 1995. IL-12 increases resistance of BALB/c mice to *Mycobacterium tuberculosis* infection. *J. Immunol.* 155: 2515–2524.
14. Ulrichs, T., G. A. Kosmiadi, V. Trusov, S. Jörg, L. Pradl, M. Titukhina, V. Mishenko, N. Gushina, and S. H. E. Kaufmann. 2004. Human tuberculous granulomas induce peripheral lymphoid follicle-like structures to orchestrate local host defence in the lung. *J. Pathol.* 204: 217–228.
15. Ordway, D., M. Harton, M. Henao-Tamayo, R. Montoya, I. M. Orme, and M. Gonzalez-Juarrero. 2006. Enhanced macrophage activity in granulomatous lesions of immune mice challenged with *Mycobacterium tuberculosis*. *J. Immunol.* 176: 4931–4939.
16. Ordway, D., M. Henao-Tamayo, I. M. Orme, and M. Gonzalez-Juarrero. 2005. Foamy macrophages within lung granulomas of mice infected with *Mycobacterium tuberculosis* express molecules characteristic of dendritic cells and antiapoptotic markers of the TNF receptor-associated factor family. *J. Immunol.* 175: 3873–3881.
17. Pedrosa, J., B. M. Saunders, R. Appelberg, I. M. Orme, M. T. Silva, and A. M. Cooper. 2000. Neutrophils play a protective nonphagocytic role in systemic *Mycobacterium tuberculosis* infection of mice. *Infect. Immun.* 68: 577–583.
18. Rook, G. A. W., R. Hernandez-Pando, K. Dheda, and G. Teng Seah. 2004. IL-4 in tuberculosis: implications for vaccine design. *Trends Immunol.* 25: 483–488.
19. Turner, J., M. Gonzalez-Juarrero, D. L. Ellis, R. J. Basaraba, A. Kipnis, I. M. Orme, and A. M. Cooper. 2002. In vivo IL-10 production reactivates chronic pulmonary tuberculosis in C57BL/6 mice. *J. Immunol.* 169: 6343–6351.
20. Dheda, K., H. Booth, J. F. Huggett, M. A. Johnson, A. Zumla, and G. A. W. Rook. 2005. Lung remodeling in pulmonary tuberculosis. *J. Infect. Dis.* 192: 1201–1210.
21. Quinn, K. M., R. S. McHugh, F. J. Rich, L. M. Goldsack, G. W. de Lisle, B. M. Buddle, B. Delahunt, and J. R. Kirkman. 2006. Inactivation of CD4$^+$ CD25$^+$ regulatory T cells during early mycobacterial infection increases cytokine production but does not affect pathogen load. *Immunol. Cell Biol.* 84: 467–474.
22. Guyot-Revol, V., J. A. Innes, S. Hackforth, T. Hinks, and A. Lalvani. 2006. Regulatory T cells are expanded in blood and disease sites in patients with tuberculosis. *Am. J. Respir. Crit. Care Med.* 173: 803–810.
23. Valway, S. E., M. P. C. Sanchez, T. F. Shinnick, I. Orme, T. Agerton, D. Hoy, J. S. Jones, H. Westmoreland, and I. M. Onorato. 1998. An outbreak involving extensive transmission of a virulent strain of *Mycobacterium tuberculosis*. *N. Engl. J. Med.* 338: 633–639.
24. Gavin, M. A., J. P. Rasmussen, J. D. Fontenot, V. Vasta, V. C. Manganiello, J. A. Beavo, and A. Y. Rudensky. 2007. Foxp3-dependent programme of regulatory T-cell differentiation. *Nature* 445: 771–774.
25. Jonuleit, H., and E. Schmitt. 2003. The regulatory T cell family: distinct subsets and their interrelations. *J. Immunol.* 171: 6323–6327.
26. Banz, A., A. Peixoto, C. Pontoux, C. Cordier, B. Rocha, and M. Papiernik. 2003. A unique subpopulation of CD4$^+$ regulatory T cells controls wasting disease, IL-10 secretion and T cell homeostasis. *Eur. J. Immunol.* 33: 2419–2428.
27. Ramsdell, F. 2003. Foxp3 and natural regulatory T cells: key to a cell lineage? *Immunity* 19–25.
28. Oldenhove, G., M. de Heusch, G. Urbain-Vansanten, J. Urbain, C. Maliszewski, O. Leo, and M. Moser. 2003. CD4$^+$CD25$^+$ regulatory T cells control T helper cell type 1 responses to foreign antigens induced by mature dendritic cells in vivo. *J. Exp. Med.* 198: 259–266.

29. Sakaguchi, S., M. Ono, R. Setoguchi, H. Yagi, S. Hori, Z. Fehervari, J. Shimizu, T. Takahashi, and T. Nomura. 2006. Foxp3$^+$CD25$^+$CD4$^+$ natural regulatory T cells in dominant self-tolerance and autoimmune disease. *Immunol. Rev.* 212: 8–27.
30. Sakaguchi, S. 2005. Naturally arising Foxp3-expressing CD25$^+$CD4$^+$ regulatory T cells in immunological tolerance to self and non-self. *Nat. Immunol.* 6: 345–353.
31. Wu, Y., Q. H. Wang, L. Zheng, H. Feng, J. Liu, S. H. Ma, and Y. M. Cao. 2007. *Plasmodium yoelii*: distinct CD4$^+$CD25$^+$ regulatory T cell responses during the early stages of infection in susceptible and resistant mice. *Exp. Parasitol.* 115: 301–304.
32. Gasper-Smith, N., I. Marriott, and K. L. Bost. 2006. Murine gamma-herpesvirus 68 limits naturally occurring CD4$^+$CD25$^+$ T regulatory cell activity following infection. *J. Immunol.* 177: 4670–4678.
33. Zelinskyy, G., A. R. Kraft, S. Schimmer, T. Arndt, and U. Dittmer. 2006. Kinetics of CD8$^+$ effector T cell responses and induced CD4$^+$ regulatory T cell responses during friend retrovirus infection. *Eur. J. Immunol.* 36: 2658–2670.
34. Franzese, O., P. T. F. Kennedy, A. J. Gehring, J. Gotto, R. Williams, M. K. Maini, and A. Bertoletti. 2005. Modulation of the CD8$^+$ T-cell response by CD4$^+$ CD25$^+$ regulatory T cells in patients with hepatitis B virus infection. *J. Virol.* 79: 3322–3328.
35. De Luca, A., M. De Falco, S. Iaquinto, and G. Iaquinto. 2004. Effects of *Helicobacter pylori* infection on cell cycle progression and the expression of cell cycle regulatory proteins. *J. Cell Physiol.* 200: 334–342.
36. Joshi, S. G., C. W. Francis, D. J. Silverman, and S. K. Sahni. 2004. NF-κb activation suppresses host cell apoptosis during *Rickettsia rickettsii* infection via regulatory effects on intracellular localization or levels of apoptogenic and anti-apoptotic proteins. *FEMS Microb. Lett.* 234: 333–341.
37. Accapezzato, D., V. Francavilla, M. Paroli, M. Casciaro, L. V. Chircu, A. Cividini, S. Abrignani, M. U. Mondelli, and V. Barnaba. 2004. Hepatic expansion of a virus-specific regulatory CD8$^+$ T cell population in chronic hepatitis C virus infection. *J. Clin. Invest.* 113: 963–972.
38. Xu, D., H. Liu, M. Komai-Koma, C. Campbell, C. McSharry, J. Alexander, and F. Y. Liew. 2003. CD4$^+$CD25$^+$ regulatory T cells suppress differentiation and functions of Th1 and Th2 cells: *Leishmania major* infection, and colitis in mice. *J. Immunol.* 170: 394–399.
39. McKee, A. S., and E. J. Pearce. 2004. CD25$^+$CD4$^+$ cells contribute to Th2 polarization during helminth infection by suppressing Th1 response development. *J. Immunol.* 173: 1224–1231.
40. Long, T. T., S. Nakazawa, S. Onizuka, M. C. Huaman, and H. Kanbara. 2003. Influence of CD4$^+$CD25$^+$ T cells on *Plasmodium berghei* NK65 infection in BALB/c mice. *Int. J. Parasitol.* 33: 175–183.
41. Belkaid, Y., R. B. Blank, and I. Suffia. 2006. Natural regulatory T cells and parasites: a common quest for host homeostasis. *Immunol. Rev.* 212: 287–300.
42. Belkaid, Y., and B. T. Rouse. 2005. Natural regulatory T cells in infectious disease. *Nat. Immunol.* 6: 353–360.
43. Asselin-Paturel, C., and G. Trinchieri. 2005. Production of type I interferons: plasmacytoid dendritic cells and beyond. *J. Exp. Med.* 202: 461–465.
44. Dalod, M., T. P. Salazar-Mather, L. Malmgaard, C. Lewis, C. Asselin-Paturel, F. Briere, G. Trinchieri, and C. A. Biron. 2002. Interferon α/β and interleukin-12 responses to viral infections: pathways regulating dendritic cell cytokine expression in vivo. *J. Exp. Med.* 195: 517–528.
45. Stetson, D. B., and R. Medzhitov. 2006. Type I interferons in host defense. *Immunity* 25: 373–381.
46. Taylor, J. L., D. J. Ordway, J. Troudt, M. Gonzalez-Juarrero, R. J. Basaraba, and I. M. Orme. 2005. Factors associated with severe granulomatous pneumonia in *Mycobacterium tuberculosis*-infected mice vaccinated therapeutically with HSP65 DNA. *Infect. Immun.* 73: 5189–5193.
47. Nocentini, G., and C. Riccardi. 2005. GITR: a multifaceted regulator of immunity belonging to the tumor necrosis factor receptor superfamily. *Eur. J. Immunol.* 35: 1016–1022.
48. Shevach, E. M., and G. L. Stephens. 2006. The GITR-GITRL interaction: co-stimulation or contrasuppression of regulatory activity? *Nat. Rev. Immunol.* 6: 613–618.
49. Baumgartner-Nielsen, J., C. Vestergaard, K. Thestrup-Pedersen, M. Deleuran, and B. Deleuran. 2006. Glucocorticoid-induced tumour necrosis factor receptor (GITR) and its ligand (GITRL) in atopic dermatitis. *Acta Derm. Venereol.* 86: 393–398.
50. Asselin-Paturel, C., A. Boonstra, M. Dalod, I. Durand, N. Yessaad, C. Dezutter-Dambuyant, A. Vicari, A. O'Garra, C. Biron, F. Brière, and G. Trinchieri. 2001. Mouse type I IFN-producing cells are immature APCs with plasmacytoid morphology. *Nat. Immunol.* 2: 1114–1150.
51. Auerbuch, V., D. G. Brockstedt, N. Meyer-Morse, M. O'Riordan, and D. A. Portnoy. 2004. Mice lacking the type I interferon receptor are resistant to *Listeria monocytogenes*. *J. Exp. Med.* 200: 527–533.
52. Kursar, M., M. Koch, H.-W. Mittrucker, G. Nouailles, K. Bonhagen, T. Kamradt, and S. H. E. Kaufmann. 2007. Cutting edge: Regulatory T cells prevent efficient clearance of *Mycobacterium tuberculosis*. *J. Immunol.* 178: 2661–2665.
53. Higgins, S. C., E. C. Lavelle, C. McCann, B. Keogh, E. McNeela, P. Byrne, B. O'Gorman, A. Jarnicki, P. McGuirk, and K. H. G. Mills. 2003. Toll-like receptor 4-mediated innate IL-10 activates antigen-specific regulatory T cells and confers resistance to *Bordetella pertussis* by inhibiting inflammatory pathology. *J. Immunol.* 171: 3119–3127.
54. Gazzola, L., C. Tincati, A. Gori, M. Saresella, I. Marventano, and F. Zanini. 2006. Foxp3 mRNA expression in regulatory T cells from patients with tuberculosis. *Am. J. Respir. Crit. Care Med.* 174: 356–367.